



# Effect of initial biomass-specific photon supply rate on fatty acid accumulation in nitrogen depleted *Nannochloropsis gaditana* under simulated outdoor light conditions

Jorijn H. Janssen<sup>a,\*</sup>, Jasper L.S.P. Driessen<sup>a</sup>, Packo P. Lamers<sup>a</sup>, René H. Wijffels<sup>a,b</sup>, Maria J. Barbosa<sup>a,c</sup>

<sup>a</sup> Bioprocess Engineering, AlgaePARC, Wageningen University and Research, P.O. Box 16, 6700 AA Wageningen, the Netherlands

<sup>b</sup> Nord University, Faculty of Biosciences and Aquaculture, N-8049 Bodø, Norway

<sup>c</sup> University of Bergen, Department of Biology, PO Box 7803, 5006 Bergen, Norway



## ARTICLE INFO

### Keywords:

*Nannochloropsis gaditana*  
Triacylglycerol  
Nitrogen starvation  
Biomass-specific photon supply rate  
Initial biomass concentration

## ABSTRACT

Triacylglycerol (TAG) accumulation in the microalgae *Nannochloropsis gaditana* is induced by nitrogen starvation and dependent on the light supplied. We studied under simulated outdoor light conditions the effect of supplied light on the TAG yield by varying the biomass-specific photon supply rate present at the onset of nitrogen starvation. High, intermediate and low average biomass-specific photon supply rates (26, 11 and 6  $\mu\text{mol g}^{-1} \text{s}^{-1}$ ) were achieved by applying equal incident light intensity to different biomass concentrations (1.2, 2.9 and 5.4  $\text{g L}^{-1}$ ). The intermediate biomass-specific photon supply rate resulted in the highest time-averaged TAG yield on light; 0.09  $\text{g}_{\text{TAG}} \text{mol}_{\text{ph}}^{-1}$ . Sub-optimal yields were attributed to photosaturation, photoinhibition, light falling through reactor without being absorbed and high maintenance requirements. The biomass-specific photon supply rate is important to optimize TAG production by microalgae.

## 1. Introduction

Due to the increasing world population, the demands for food and energy are rising the need for alternative, sustainable sources for food-commodities and fuels increases [1]. Triacylglycerol (TAG) has a wide range of applications and is used in the food- and petrochemical industry. Microalgae can be used as sustainable alternative for TAG production. For this, the production process should be optimized to be economically feasible and compete with plant-based and fossil oils [2]. Nitrogen starvation is the most applied technique for TAG accumulation in microalgae [3]. *Nannochloropsis* is a marine microalgae species which accumulates large amounts of TAG (up to 54% per dry weight) upon nitrogen starvation and produces the omega-3 fatty acid eicosapentaenoic acid (EPA) [4,5]. Nitrogen starvation is often applied in a two phase batch strategy in which the microalgae are first grown under non-limiting conditions followed by nitrogen starvation to induce TAG accumulation.

Under identical light intensities, low biomass concentration results in a high biomass-specific photon supply rate and a high biomass concentration results in a low biomass-specific photon supply rate. Light supply rate is important as it affects the photosynthetic rate and

thereby the biomass and TAG yields. In outdoor cultivation, for a given cultivation system and light intensity, the biomass-specific photon supply rate can be changed by changing the biomass concentration inside the reactor. Biomass concentration dictates the light gradient inside the photobioreactor and, at a fixed light intensity, also the biomass-specific photon supply rate. There are different processes which influence the photosystems and photosynthetic rates: photosaturation, photoinhibition and photoacclimation. When suboptimal biomass-specific photon supply rates are used, these processes can lead to sub-optimal TAG yields (Fig. 1).

One of these processes is photosaturation. At light intensities higher than the photosynthetic processing capacity, photosynthesis is saturated and the excess energy is dissipated as heat, thereby decreasing photosynthetic efficiency [6]. Another process is photoinhibition, which is the process where excess of photons elicit formation of oxygen radicals (ROS) which damage key proteins in the photosynthetic machinery and thereby decrease photosynthetic efficiency and thus increase photosaturation [7]. Microalgae can also adapt their pigmentation dependent on the light intensity received through photoacclimation and thereby adapt their photosynthetic efficiency [7].

In addition to the processes affecting the photosystems and

\* Corresponding author.

E-mail address: [jorijn.janssen@wur.nl](mailto:jorijn.janssen@wur.nl) (J.H. Janssen).

<https://doi.org/10.1016/j.algal.2018.10.002>

Received 5 July 2018; Received in revised form 28 August 2018; Accepted 2 October 2018

Available online 09 October 2018

2211-9264/ © 2018 The Authors. Published by Elsevier B.V. This is an open access article under the CC BY-NC-ND license (<http://creativecommons.org/licenses/by-nc-nd/4.0/>).

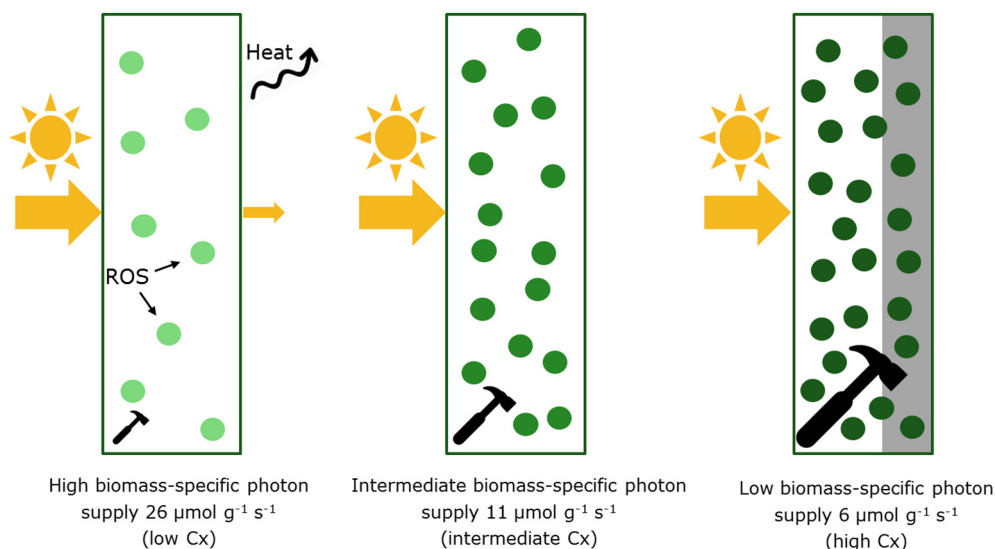


**Fig. 1.** Schematic overview of different biomass-specific photon supply rates and the processes expected to influence the TAG yield. The size of the hammer represents the volumetric maintenance energy requirements.

photosynthetic efficiency, TAG yield on light will also be affected by the metabolic processes downstream of light absorption; TAG yield decreases when absorbed light energy is used for other processes than TAG production. For instance, light energy is necessary for cell maintenance, which are non-growth related processes (e.g. turnover of cellular materials or maintain concentration gradients across cell membranes) [8,9]. The volumetric energy requirement for cell maintenance is dependent on the biomass concentration [10]. When there is not enough light energy supplied for maintenance, cells need to degrade storage products such as TAG to generate energy to maintain themselves, leading to a lower TAG yield. Another factor contributing to a low TAG yield on light, but now under high biomass-specific photon supply rates, is the loss of light that goes through the reactor without being absorbed.

Previous outdoor studies showed that the amount of biomass at the start of nitrogen starvation affected TAG yield on light for *Chlorella zofingiensis* [11,12]. Increasing initial biomass concentration showed increased lipid productivity for the biomass concentrations tested (0.02, 0.15, 0.35 and 0.5 g L<sup>-1</sup>) with a reactor depth of 17 cm at varying outdoor light conditions [11]. In lab-scale experiments, no significant effect of biomass-specific photon supply rate at the start of nitrogen starvation on the overall TAG production for *Chlorella zofingiensis* was found between the tested biomass-specific photon absorption rates 4.7, 3.5 and 2.9 μmol g<sup>-1</sup> s<sup>-1</sup> using continuous light conditions [13]. For *Nannochloropsis oculata* a maximum TAG productivity under continuous light conditions was found at 13 μmol g<sup>-1</sup> s<sup>-1</sup> [14].

In this research, the effect of the biomass-specific photon supply rate on TAG yield in *Nannochloropsis gaditana* during nitrogen starvation was studied at lab-scale under simulated outdoor light conditions. Simulated outdoor light conditions were used at lab-scale to be more representative of outdoors conditions. The different biomass-specific photon supply rates were set by applying equal light intensities to different biomass concentrations present at the moment of nitrogen starvation. The outdoor light intensity was simulated using a half-sinus incident light intensity curve with a peak at noon of 1500 μmol m<sup>-2</sup> s<sup>-1</sup> and a day: night cycle of 16: 8 h. The average initial biomass-specific photon supply rates were; 26, 11 and 6 μmol g<sub>dw</sub><sup>-1</sup> s<sup>-1</sup> at the start of nitrogen starvation. This required initial biomass concentrations of 1.2, 3.0 and 5.4 g L<sup>-1</sup>. It was hypothesized that there is an optimal biomass concentration and thus biomass-specific photon supply rate at the start of nitrogen starvation where the TAG yield on light is maximal. Besides TAG, the omega-3 fatty acid eicosapentaenoic acid (EPA) was studied in

more depth. EPA is a fatty acid present in the photosynthetic membranes and TAG, and therefore differences are expected at different biomass-specific photon supply rates.

## 2. Materials and methods

### 2.1. Strain, cultivation medium and pre-cultivation

The microalgae *Nannochloropsis gaditana* CCFM-01 was obtained from the Microalgae Collection of Fitoplankton Marino S.L. Pre-cultures of *N. gaditana* were kept in 250 mL Erlenmeyer flasks with 100 mL culture, incubated at 25 °C in an orbital shaker incubator (125 rpm). The cultures were maintained at low light conditions (30–40 μmol m<sup>-2</sup> s<sup>-1</sup>), in a 16:8 h day:night cycle. A week before inoculation, the microalgae were transferred to continuous high light conditions (118 μmol m<sup>-2</sup> s<sup>-1</sup>) with air enriched with 2.5% CO<sub>2</sub> for inoculum production. The growth medium was based on [15] and contained: NaCl 445 mM; KNO<sub>3</sub> 33.6 mM; Na<sub>2</sub>SO<sub>4</sub> 3.5 mM; MgSO<sub>4</sub>·7H<sub>2</sub>O 3 mM; CaCl<sub>2</sub>·2H<sub>2</sub>O 2.5 mM; K<sub>2</sub>HPO<sub>4</sub> 2.5 mM; NaFeEDTA 28 μM; Na<sub>2</sub>EDTA·2H<sub>2</sub>O 80 μM; MnCl<sub>2</sub>·4H<sub>2</sub>O 19 μM; ZnSO<sub>4</sub>·7H<sub>2</sub>O 4 μM; CoCl<sub>2</sub>·6H<sub>2</sub>O 1.2 μM; CuSO<sub>4</sub>·5H<sub>2</sub>O 1.3 μM; Na<sub>2</sub>MoO<sub>4</sub>·2H<sub>2</sub>O 0.1 μM; Biotin 0.1 μM; vitamin B1 3.3 μM; vitamin B12 0.1 μM; and 10 mM NaHCO<sub>3</sub>. For nitrogen depleted growth medium KNO<sub>3</sub> was replaced with 33.6 mM KCl to keep equal osmolarity. Since the nitrate and phosphate concentration in the medium was high enough for a biomass concentration of approximately 5 g L<sup>-1</sup> extra nitrate and phosphate were added before it became limited during the growth phase. For the intermediate concentration (2.9 g L<sup>-1</sup>) 2.8 g KNO<sub>3</sub> was added at day 7 of the growth phase. For the high biomass concentration (5.4 g L<sup>-1</sup>) 2.6 g KNO<sub>3</sub> was added at day 7 and 4.8 g KNO<sub>3</sub> and 0.6 g K<sub>2</sub>HPO<sub>4</sub> were added at day 13 of the growth phase. During pre-cultivation in Erlenmeyer flasks 100 mM 4-(2-hydroxyethyl)piperazine-1-ethanesulfonic acid (HEPES) was added as pH buffer. The pH of the growth media was adjusted to pH 7.5 and filter sterilized prior to use (pore size, 0.2 μm).

### 2.2. Photobioreactor and experimental setup

Experiments were performed in an aseptic, heat-sterilized, flat-panel, airlift-loop photobioreactor (Labfors 5 Lux, Infors HT, Switzerland, 2010) with a working volume of 1.8 L and a reactor depth of 20.7 mm. Mixing was provided by aeration of the culture with 1 L min<sup>-1</sup> filtered air mixed with 2% CO<sub>2</sub>. The pH was maintained at

7.5 by on-demand addition of 2.5% (v/v) sulphuric acid. Temperature was controlled at 26 °C by recirculation of water through a water jacket in direct contact with the cultivation chamber at the back of the reactor and connected to a cryostat. The incident light intensity was controlled and provided by 260 high power LED lights (28 V, 600 W) at the culture side of the reactor. The reactor chamber was isolated to prevent interference of ambient light. *Nannochloropsis gaditana* was grown in a two-step batch process using growth phase followed by nitrogen starvation to induce TAG accumulation. In the growth phase, microalgae were inoculated at biomass concentration 0.09–0.12 g L<sup>-1</sup> in nitrogen replete medium. After growth the cells were harvested by centrifugation (800 g, 25 min) and washed with nitrogen deplete medium to remove the residual nitrogen and re-inoculated in nitrogen depleted medium, starting the nitrogen starvation phase. The microalgae were grown up 2.6, 5.0 and 7.4 g L<sup>-1</sup> and diluted back to 1.2, 2.9 and 5.4 g L<sup>-1</sup>, respectively, at the beginning of the nitrogen starvation phase. The dilutions were kept as small as possible to prevent a large change in biomass-specific photon supply rate after washing and starting the nitrogen starvation of the culture.

During the growth phase the microalgae were subjected to a 16:8 h day:night cycle with constant light intensity during the day (block light cycle). The light intensity was increased stepwise keeping the outgoing light around 30–40 μmol m<sup>-2</sup> s<sup>-1</sup>. Once a light intensity of 636 μmol m<sup>-2</sup> s<sup>-1</sup> was reached, the block light cycle was changed into a sinusoidal light cycle during the day as used by [16] simulating a summer day in the Netherlands. The equation:  $I(t) = I_{max} * \sin(t / P * \pi)$  shows the sinusoidal light cycle applied during the day with I (t) (in μmol m<sup>-2</sup> s<sup>-1</sup>) the light intensity at time t (in hours); t is the number of hours after sunrise; I<sub>max</sub> is the light intensity at solar noon (1500 μmol m<sup>-2</sup> s<sup>-1</sup>); P is the duration of the light period (16 h). During the night, 16 to 24 h after sunrise, no light was supplied. The light was maintained equal throughout the rest of the experiment. This light regime was maintained for at least 1 day during the growth phase before cells were centrifuged to start the nitrogen starvation phase. By setting different biomass concentrations at the start of nitrogen starvation the biomass-specific photon supply rate was set. The lowest biomass concentration has the highest biomass-specific photon supply rate. The biomass-specific photon supply rate was calculated by dividing the average light intensity supplied over the light period by the biomass concentration at the start of the nitrogen starvation phase. The initial biomass concentrations and corresponding average biomass-specific photon supply rates at the moment of nitrogen starvation are shown in Table 1.

### 2.3. Offline measurements

During the experiment, daily samples were taken from the photobioreactor to monitor the growth and photosynthetic activity of the microalgal biomass. The optical density (OD) was measured at 750 nm using a UV-VIS spectrophotometer (Hach Lange DR-6000, light path 1 cm). The dry weight was measured in triplicate by filtering (Whatman, 55 mm) and drying of biomass samples overnight at 100 °C as described by [17] with the exception that ammonium formate (0.5 M) was used for dilution and washing. Since the supernatant was

**Table 1**

Biomass concentration at start of nitrogen starvation and the corresponding average biomass-specific photon supply rate.

Biomass-specific photon supply rate	Biomass concentration at start of nitrogen starvation (g L <sup>-1</sup> )	Average biomass-specific photon supply rate (μmol <sub>ph</sub> g <sub>dw</sub> <sup>-1</sup> s <sup>-1</sup> )
High (■)	1.2	26
Intermediate (▲)	2.9	11
Low (◊)	5.4	6

turbid reddish after centrifugation the dry weight of the supernatant was subtracted from the dry weight and also used for the other analyses. The cell concentration was measured in duplicate with the Multisizer II (Beckman Coulter) using a 50 μm aperture tube. Isotone II diluent was used to dilute the samples before measuring.

The photosystem II (PSII) maximal quantum yield (F<sub>v</sub>/F<sub>m</sub>) was measured by the chlorophyll *a* fluorescence at 455 nm using a fluorometer (AquaPen-C AP-C100, Photon Systems Instruments, Czech Republic) and calculated according to [18]. Samples were diluted to OD750 0.3 and dark-adapted for 15 min at room temperature before measurement.

The dry weight-specific optical cross section was measured using a spectrophotometer (Shimadzu UV-2600, Japan), equipped with an integrating sphere, to measure light absorption between 400 and 750 nm. The dry weight specific optical cross section (m<sup>2</sup> kg<sup>-1</sup>) was calculated according to [19]. Samples were diluted to approximately OD 750 of 0.3 prior to measurement and transferred in cuvettes (100.099-OS, Hellma Germany; light path: 2 mm). To calculate the volumetric optical cross section, the dry weight-specific optical cross section was multiplied with the dry weight concentration in the photobioreactor.

### 2.4. Fatty acid analysis

Biomass samples were centrifuged, washed twice with ammonium formate (0.5 M), stored at -20 °C and lyophilized. Lipids were extracted, separated and quantified according to [15,20]. In short, cells were disrupted using a beat beater and lipids were extracted using a mixture of chloroform:methanol (1:1.25, v:v) with triptadecanoic (T4257, Sigma Aldrich) and 1,2-dipentadecanoyl-*sn*-glycero-3-[Phospho-rac-(1-glycerol)] (sodium salt) (840446P, Avanti Polar Lipids Inc.) as internal standard for the TAG and polar membrane lipid fraction, respectively. The TAGs were separated from the polar membrane lipids by solid phase extraction (Sep-Pak Vac 6cc, Waters) using different eluents. The fatty acids were methylated by incubation with methanol with 5% H<sub>2</sub>SO<sub>4</sub> for 3 h at 70 °C and extracted with hexane. The fatty acid methyl esters were identified and quantified using gas chromatography (GC-FID) [15]. The total TAG and polar membrane lipid content was calculated as a sum of the individual fatty acids of these fractions.

### 2.5. Calculation time-averaged TAG yield on light

The time-averaged TAG yield on light was calculated according to [21]. The TAG produced over a certain time period was divided by the light supplied during that period. This light included the light necessary for inoculum production, using a theoretical biomass yield on light of 1 g mol<sub>ph</sub><sup>-1</sup>. It is important to consider the energy necessary for inoculum production especially when using high starting biomass concentrations.

## 3. Results and discussion

The nitrogen starvation experiments were performed at high (26 μmol<sub>ph</sub> g<sub>dw</sub><sup>-1</sup> s<sup>-1</sup>), intermediate (11 μmol<sub>ph</sub> g<sub>dw</sub><sup>-1</sup> s<sup>-1</sup>) and low (6 μmol<sub>ph</sub> g<sub>dw</sub><sup>-1</sup> s<sup>-1</sup>) biomass-specific photon supply rates by using a low (1.2 g L<sup>-1</sup>), intermediate (2.9 g L<sup>-1</sup>) and high (5.4 g L<sup>-1</sup>) biomass concentrations at the start of nitrogen starvation, respectively. All results are shown from the start of nitrogen starvation.

### 3.1. Biomass concentration

From the onset of nitrogen starvation, biomass concentration was measured by dry weight (g L<sup>-1</sup>) and cell concentration (cells mL<sup>-1</sup>) (Fig. 2).

The biomass production rates were on average 0.3, 0.8 and 0.5 g<sub>dw</sub> L<sup>-1</sup> day<sup>-1</sup> for high, intermediate and low initial biomass-specific photon supply rates, respectively, during the first 5 days of

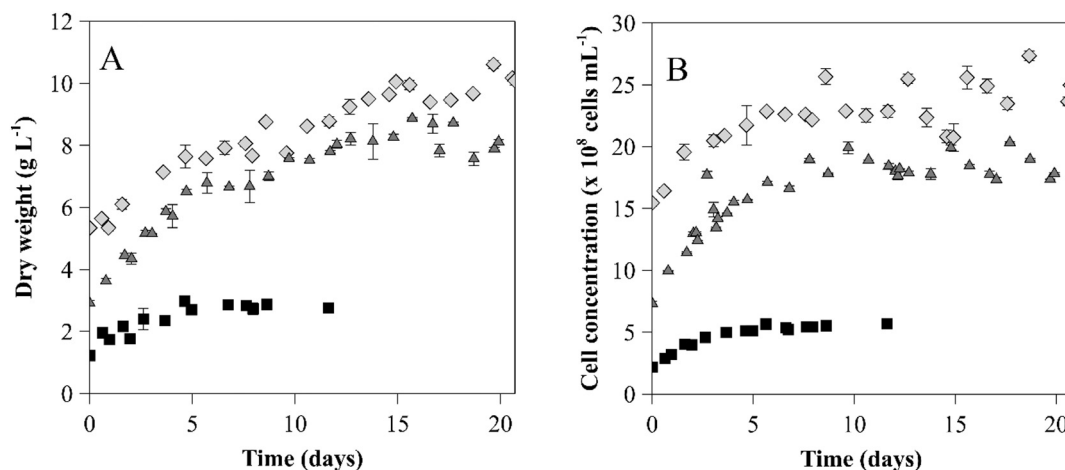


**Fig. 2.** Dry weight concentration ( $\text{g L}^{-1}$ ) (A) and cell concentration ( $\text{cells mL}^{-1}$ ) (B) for high (■), intermediate ( $\Delta$ ) and low ( $\diamond$ ) biomass-specific photon supply rate at the start of nitrogen starvation (time = 0). The error bars show the standard deviation of triplicate dry weight measurements and the absolute deviation of duplicate measurements for the cell concentration.

nitrogen starvation (Fig. 2A). Showing the highest biomass production rate for the intermediate biomass-specific photon supply rate.

Similar to the dry weight results, the intermediate biomass-specific photon supply rate showed the highest increase in cell concentration and thus most cell division during the first 5 days of nitrogen starvation (Fig. 2B).

### 3.2. Lipid accumulation

The TAG content at the intermediate biomass-specific photon supply rate increased faster compared to high biomass-specific photon supply rate during the first 5 days of nitrogen starvation ( $0.05 \text{ g}_{\text{TAG}} \text{ g}_{\text{dw}}^{-1} \text{ day}^{-1}$  compared to  $0.03 \text{ g}_{\text{TAG}} \text{ g}_{\text{dw}}^{-1} \text{ day}^{-1}$ ) (Fig. 3A).

For the low biomass-specific photon supply rate the TAG content increased slower ( $0.01 \text{ g}_{\text{TAG}} \text{ g}_{\text{dw}}^{-1} \text{ day}^{-1}$ ).

Similar to the increase in TAG content, the TAG concentration in the reactor increased the fastest for the intermediate biomass-specific photon supply rate and reached the highest TAG concentration (Fig. 3B). The average TAG production rates were  $0.12$ ,  $0.33$  and  $0.08 \text{ g L}^{-1} \text{ day}^{-1}$  over the first 5 days of nitrogen starvation for high, intermediate and low biomass-specific photon supply rates.

The polar lipid content was  $0.09$ ,  $0.12$  and  $0.18 \text{ g}_{\text{dw}}^{-1}$  for the high, intermediate and low biomass-specific photon supply rates at the start of nitrogen starvation (Fig. 3C). Showing the highest polar lipid content for the lowest biomass-specific photon supply rate.

The maximal time-averaged TAG yield on light was  $0.05$ ;  $0.09$  and

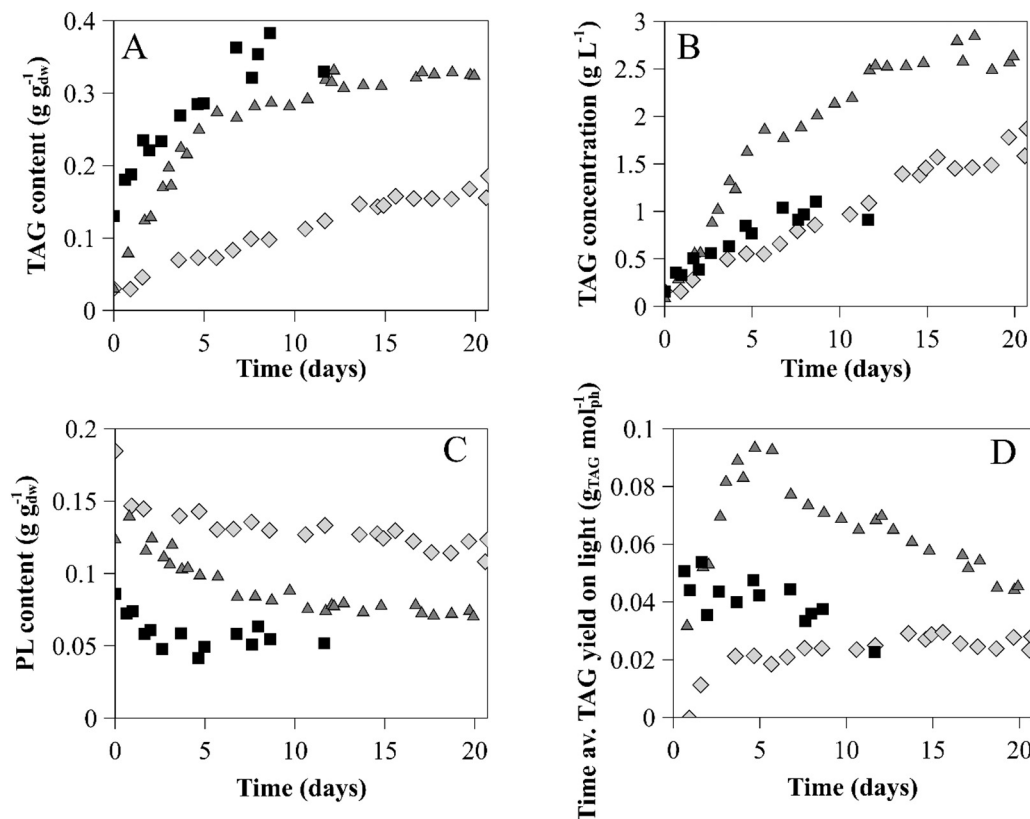


**Fig. 3.** TAG content expressed per dry biomass ( $\text{g}_{\text{TAG}} \text{ g}_{\text{dw}}^{-1}$ ) (A), TAG concentration ( $\text{g}_{\text{TAG}} \text{ L}^{-1}$ ) (B), polar lipid content expressed per dry biomass ( $\text{g}_{\text{PL}} \text{ g}_{\text{dw}}^{-1}$ ) (C) and the time-averaged TAG yield on light ( $\text{g}_{\text{TAG}} \text{ mol}_{\text{ph}}^{-1}$ ) (D) for high (■), intermediate ( $\Delta$ ) and low ( $\diamond$ ) biomass-specific photon supply rates at the start of nitrogen starvation (time = 0).

$0.02 \text{ g}_{\text{TAG}} \text{ mol}_{\text{ph}}^{-1}$  (values not corrected for inoculum production are: 0.07; 0.12 and  $0.03 \text{ g}_{\text{TAG}} \text{ mol}_{\text{ph}}^{-1}$ ) for high, intermediate and low biomass-specific photon supply rates (Fig. 3D). These maximal time-averaged TAG yield on light were achieved after 2, 5 and 4 days of nitrogen starvation for the high, intermediate and low biomass-specific photon supply rates, respectively. The highest time-averaged TAG yield on light ( $0.09 \text{ g}_{\text{TAG}} \text{ mol}_{\text{ph}}^{-1}$ ) was achieved at the intermediate initial biomass-specific photon supply rate ( $11 \mu\text{mol}_{\text{ph}} \text{ g}_{\text{dw}}^{-1} \text{ s}^{-1}$ ). This maximal time-averaged TAG yield on light was similar to  $0.10 \text{ g}_{\text{TAG}} \text{ mol}_{\text{ph}}^{-1}$  achieved for *Nannochloropsis* sp. cultivated under the same sinusoidal day night light regime using a biomass-specific photon supply rate of  $16 \mu\text{mol}_{\text{ph}} \text{ g}_{\text{dw}}^{-1} \text{ s}^{-1}$  [16]. This is biomass-specific photon supply rate between the high and intermediate biomass-specific photon supply rates used in this study (26 and  $11 \mu\text{mol}_{\text{ph}} \text{ g}_{\text{dw}}^{-1} \text{ s}^{-1}$ ). Our results are in line with the maximal TAG productivity which was achieved for *Nannochloropsis oculata* at a biomass-specific supply rate of  $13 \mu\text{mol} \text{ g}^{-1} \text{ s}^{-1}$  under continuous light conditions [14]. On the contrary, [13] found no difference in TAG yield on light for *Chlorella zofingiensis* within the tested range of biomass-specific photon absorption rates (2.9, 3.5 and  $4.7 \mu\text{mol} \text{ g}^{-1} \text{ s}^{-1}$ ) under continuous light. In the present study, however, a broader biomass-specific photon supply rate range (6, 11 and  $26 \mu\text{mol} \text{ g}_{\text{dw}}^{-1} \text{ s}^{-1}$ ) and simulated outdoor light conditions were used. Therefore, sub-optimal yields for both lower and higher biomass-specific photon supply rates could be measured.

### 3.3. Photosynthetic capacity

Nitrogen starved *Nannochloropsis gaditana* relies on photosynthesis to support *de novo* TAG synthesis [5]. Therefore, the photosystem II (PSII) maximum quantum yield and the dry weight-specific optical cross section were measured (Fig. 4).

The photosystem II (PSII) maximal quantum yield decreased for all cultures during nitrogen starvation (Fig. 4A). This was similar to results found for *Nannochloropsis oceanica* during nitrogen starvation [22,23] and indicated a reduced photosynthetic efficiency. At the start of nitrogen starvation the PSII maximal quantum yield was similar for the intermediate and high biomass-specific photon supply rates (between 0.64 and 0.67) and lower for the low biomass-specific photon supply rate (0.54).

The PSII maximal quantum yield decreased similarly for the low and intermediate biomass-specific photon supply rate. The high biomass-specific supply rate, however, decreased faster indicating more degradation or damage to PSII causing decrease in photosynthetic efficiency (Fig. 4A).

The intermediate biomass-specific photon supply rate resulted in the highest time-averaged TAG yield on light because the highest photosystem II maximum quantum yield was maintained and all light

supplied to the culture was absorbed resulting in a more efficient use of energy for TAG production. Furthermore, the biomass concentration was low enough to keep the energy required for maintenance relatively low compared to the culture with high biomass concentration (low biomass-specific photon supply rate).

The high biomass-specific photon supply rate resulted in lower TAG yield on light compared to the intermediate biomass-specific photon supply rate. This suboptimal yield could be caused by several phenomena. Firstly, the fast decrease in PSII maximal quantum yield can probably be attributed to photoinhibition, [24,25]. Photoinhibition is a process in which excess of photons damage key proteins in the photosynthetic machinery resulting in lower photosynthetic efficiency causing suboptimal TAG yield on light. At high biomass-specific photon supply rate can result in the largest excess of photons. Secondly, at the higher biomass-specific photon supply rate photosaturation can occur in a larger part of the reactor compared to the lower biomass-specific photon absorption rates and therefore dissipating more excess energy as heat. Thirdly, part of the supplied incident light fell through the reactor and was not absorbed by the microalgae and could not be used for TAG production. Approximately 8% of the incident light fell through the reactor at the peak light intensity ( $1500 \mu\text{mol} \text{ m}^{-2} \text{ s}^{-1}$ ) at the first day, without being used by the culture. At low and intermediate biomass-specific photon supply rates all supplied light was absorbed.

The lower TAG yield on light for the low biomass-specific photon supply rate, on the other hand, was probably caused by the relative high volumetric maintenance energy requirement due to high biomass concentration, assuming a constant maintenance energy per biomass for all different biomass concentrations. This energy is not available for TAG production and can therefore lead to a lower TAG yield on light. High biomass concentrations necessary for low biomass-specific supply rate also have a higher energy requirement for inoculum production which has a negative effect on overall TAG yield on light. In addition, the culture with low biomass-specific photon supply rate showed a reduced photosynthetic quantum yield at the start of nitrogen starvation, which can result in lower TAG yields on light.

The different biomass-specific photon supply rates also influence the dry weight-specific optical cross section (Fig. 4B). Microalgae can adapt their pigmentation dependent on the light received by photoacclimation. At high biomass-specific photon supply rates (low biomass concentration) the pigmentation decreases and at low biomass-specific photon supply rates (high biomass concentration) the pigmentation increases [26]. The effect of photoacclimation during the growth phase was shown by the dry weight-specific optical cross section at the start of the nitrogen starvation phase. The biomass-specific optical cross section for the high biomass-specific photon supply rates was lower ( $116 \text{ m}^2 \text{ kg}^{-1}$ ) compared to the low and intermediate biomass-specific photon supply rates (275 and  $281 \text{ m}^2 \text{ kg}^{-1}$ ).

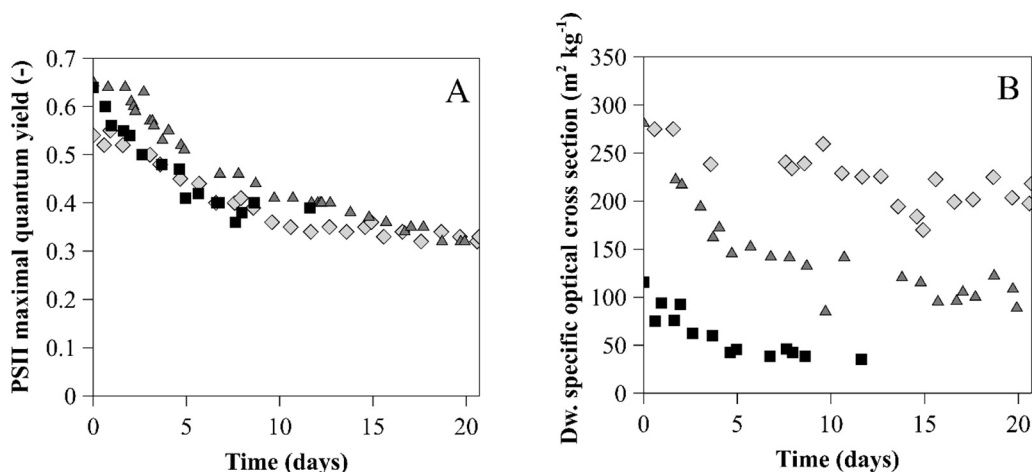
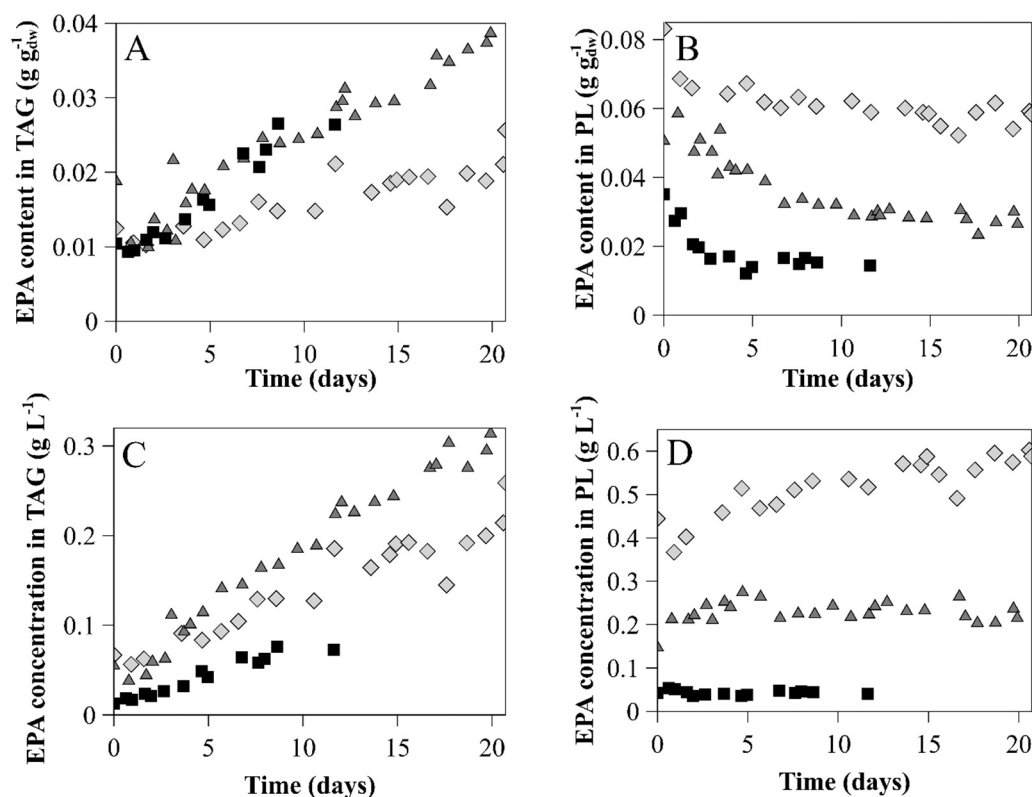


Fig. 4. Photosystem II maximal quantum yield (A) and dry weight-specific optical cross section ( $\text{m}^2 \text{ kg}^{-1}$ ) (B) for high (■), intermediate (▲) and low (◇) biomass-specific photon supply rate at the start of nitrogen starvation (time = 0).



**Fig. 5.** EPA content in TAG (A) and polar membrane lipids (PL) (B) expressed per dry biomass ( $\text{g g}_{\text{dw}}^{-1}$ ) and EPA concentration in TAG (C) and PL (D) fraction ( $\text{g L}^{-1}$ ) from the start of nitrogen starvation for high (■), intermediate (▲) and low (◇) biomass-specific photon supply rate at the start of nitrogen starvation (time = 0).

During nitrogen starvation phase, the dry weight-specific optical cross section decreased for all cultures (Fig. 4B). The volumetric optical cross section ( $\text{m}^2\text{L}^{-1}$ ) was, however, stable for the low and intermediate biomass-specific photon supply rates and increased slightly for at high biomass-specific photon supply rate. The decrease in dry weight-specific optical cross section is therefore caused by the increased of non-absorbing biomass like TAG and thus thereby decreasing optical cross section per biomass. The small increase in volumetric optical cross section for the low biomass-specific photon supply rate was probably due to the increase in biomass concentration and thereby increased pigmentation by photoacclimation.

Photoacclimation most likely results in an increase of photosynthetic membranes. At low biomass-specific photon supply rate the highest dry weight-specific optical cross section results in the highest membranes and thus highest polar lipids at the start of the nitrogen starvation phase (Fig. 3C).

EPA is one of the main fatty acids present in the polar lipid fraction. EPA content expressed per dry weight in the polar lipid fraction shows the same pattern as the total polar lipid content expressed per dry weight for the different biomass-specific photon supply rates used (Fig. 5). The EPA content in the polar lipid was the highest at low biomass-specific photon supply rate at start of nitrogen starvation probably due to photoacclimation. Interestingly, the EPA content expressed per dry weight in TAG was similar at start of nitrogen starvation for all biomass-specific photon supply rates used and increased faster for the high and intermediate biomass-specific photon supply rate. The average EPA production in both TAG and polar lipid fraction over the first 12 days of nitrogen starvation was 4.9, 20.9 and 16.4  $\text{mg L}^{-1}\text{day}^{-1}$  for the high, intermediate and low biomass-specific photon supply rates, respectively. The average EPA production rate was highest at the intermediate biomass-specific due to the increase of EPA in TAG. EPA production during nitrogen starvation is thus on the initial biomass-specific photon supply rate used.

#### 4. Conclusion

The biomass-specific photon supply rate is an important parameter to optimize TAG yield on light during nitrogen starvation. Different biomass-specific photon supply rates were obtained by using different biomass concentration at equal simulated outdoor incident light intensities, at the start of nitrogen starvation. The highest TAG yield was obtained at intermediate biomass-specific photon supply rate due to highest photosynthetic capacity and all supplied light was absorbed. Sub-optimal yield at high biomass-specific photon supply rate was attributed to non-absorbed light, photosaturation and photoinhibition. Oppositely, sub-optimal yield at low biomass-specific photon supply rate was attributed to high maintenance requirements.

#### Acknowledgements

This project has received funding from the European Union's Seventh Framework Programme for research, technological development and demonstration under grant agreement no 613588.

#### Conflicts of interest

The authors declare no conflict of interest.

#### Statement of informed consent, human/animal rights

No conflicts, informed consent, human or animal rights applicable.

#### Declaration of authors' agreement

All authors agreed to the authorship and submission of the manuscript to Algal research for peer review.

## Author contributions

JHJ, PPL, RHW and MJB conceived the research and designed the experiments. JHJ and JLSPD performed the experiments, analysed and interpreted the data. JHJ wrote the original draft. PPL, RHW and MJB supervised and edited the manuscript. All authors edited and approved the final manuscript.

## References

- [1] R.B. Draaisma, R.H. Wijffels, P.M. Slegers, L.B. Brentner, A. Roy, M.J. Barbosa, Food commodities from microalgae, *Curr. Opin. Biotechnol.* 24 (2013) 169–177, <https://doi.org/10.1016/j.copbio.2012.09.012>.
- [2] R.H. Wijffels, M.J. Barbosa, An outlook on microalgal biofuels, *Science* 329 (80) (2010) 796–799, <https://doi.org/10.1126/science.1189003>.
- [3] Q. Hu, M. Sommerfeld, E. Jarvis, M. Ghirardi, M. Posewitz, M. Seibert, A. Darzins, Microalgal triacylglycerols as feedstocks for biofuel production: perspectives and advances, *Plant J.* 54 (2008) 621–639, <https://doi.org/10.1111/j.1365-313X.2008.03492.x>.
- [4] G. Benvenuti, P.P. Lamers, G. Breuer, R. Bosma, A. Cerar, R.H. Wijffels, M.J. Barbosa, Microalgal TAG production strategies: why batch beats repeated-batch, *Biotechnol. Biofuels* 9 (2016) 64, <https://doi.org/10.1186/s13068-016-0475-4>.
- [5] D. Simionato, M.A. Block, N. La Rocca, J. Jouhet, E. Maréchal, G. Finazzi, T. Morosinotto, The response of *Nannochloropsis gaditana* to nitrogen starvation includes de novo biosynthesis of triacylglycerols, a decrease of chloroplast galactolipids, and reorganization of the photosynthetic apparatus, *Eukaryot. Cell* 12 (2013) 665–676, <https://doi.org/10.1128/EC.00363-12>.
- [6] J.M. Gordon, J.E.W. Polle, Ultrahigh bioproductivity from algae, *Appl. Microbiol. Biotechnol.* 76 (2007) 969–975, <https://doi.org/10.1007/s00253-007-1102-x>.
- [7] A. Nikolaou, P. Hartmann, A. Sciandra, B. Chachuat, O. Bernard, Dynamic coupling of photoacclimation and photoinhibition in a model of microalgal growth, *J. Theor. Biol.* 390 (2016) 61–72, <https://doi.org/10.1016/j.jtbi.2015.11.004>.
- [8] A. Richmond, Q. Hu, *Handbook of Microalgal Culture: Applied Phycology and Biotechnology*, Second edition, John Wiley and Sons, 2013, <https://doi.org/10.1002/9781118567166>.
- [9] J.W.F. Zijffers, K.J. Schippers, K. Zheng, M. Janssen, J. Tramper, R.H. Wijffels, Maximum photosynthetic yield of green microalgae in photobioreactors, *Mar. Biotechnol.* 12 (2010) 708–718, <https://doi.org/10.1007/s10126-010-9258-2>.
- [10] A.M.J. Kliphuis, A.J. Klok, D.E. Martens, P.P. Lamers, M. Janssen, R.H. Wijffels, Metabolic modeling of *Chlamydomonas reinhardtii*: energy requirements for photoautotrophic growth and maintenance, *J. Appl. Phycol.* 24 (2012) 253–266, <https://doi.org/10.1007/s10811-011-9674-3>.
- [11] P. Feng, Z. Deng, Z. Hu, L. Fan, Lipid accumulation and growth of *Chlorella zofingiensis* in flat plate photobioreactors outdoors, *Bioresour. Technol.* 102 (2011) 10577–10584, <https://doi.org/10.1016/j.biortech.2011.08.109>.
- [12] P.E. Zemke, M.R. Sommerfeld, Q. Hu, Assessment of key biological and engineering design parameters for production of *Chlorella zofingiensis* (Chlorophyceae) in outdoor photobioreactors, *Appl. Microbiol. Biotechnol.* 97 (2013) 5645–5655, <https://doi.org/10.1007/s00253-013-4919-5>.
- [13] K.J.M. Mulders, J.H. Janssen, D.E. Martens, R.H. Wijffels, P.P. Lamers, Effect of biomass concentration on secondary carotenoids and triacylglycerol (TAG) accumulation in nitrogen-depleted *Chlorella zofingiensis*, *Algal Res.* 6 (2014) 8–16, <https://doi.org/10.1016/j.algal.2014.08.006>.
- [14] R. Kandilian, J. Pruvost, J. Legrand, L. Pilon, Influence of light absorption rate by *Nannochloropsis oculata* on triglyceride production during nitrogen starvation, *Bioresour. Technol.* 163 (2014) 308–319, <https://doi.org/10.1016/j.biortech.2014.04.045>.
- [15] G. Breuer, P.P. Lamers, D.E. Martens, R.B. Draaisma, R.H. Wijffels, The impact of nitrogen starvation on the dynamics of triacylglycerol accumulation in nine microalgal strains, *Bioresour. Technol.* 124 (2012) 217–226, <https://doi.org/10.1016/j.biortech.2012.08.003>.
- [16] G. Benvenuti, R. Bosma, F. Ji, P. Lamers, M.J. Barbosa, R.H. Wijffels, Batch and semi-continuous microalgal TAG production in lab-scale and outdoor photobioreactors, *J. Appl. Phycol.* 28 (2016) 3167–3177, <https://doi.org/10.1007/s10811-016-0897-1>.
- [17] A.M.J. Kliphuis, L. de Winter, C. Vejrazka, D.E. Martens, M. Janssen, R.H. Wijffels, Photosynthetic efficiency of *Chlorella sorokiniana* in a turbulently mixed short light-path photobioreactor, *Biotechnol. Prog.* 26 (2010) 687–696, <https://doi.org/10.1002/btpr.379>.
- [18] G. Benvenuti, R. Bosma, M. Cuaresma, M. Janssen, M.J. Barbosa, R.H. Wijffels, Selecting microalgae with high lipid productivity and photosynthetic activity under nitrogen starvation, *J. Appl. Phycol.* 27 (2015) 1425–1431, <https://doi.org/10.1007/s10811-014-0470-8>.
- [19] T. de Mooij, M. Janssen, O. Cerezo-Chinarro, J.H. Mussgnug, O. Kruse, M. Ballottari, R. Bassi, S. Bujaldon, F.A. Wollman, R.H. Wijffels, Antenna size reduction as a strategy to increase biomass productivity: a great potential not yet realized, *J. Appl. Phycol.* 27 (2015) 1063–1077, <https://doi.org/10.1007/s10811-014-0427-y>.
- [20] G.M. León-Saiki, I.M. Remmers, D.E. Martens, P.P. Lamers, R.H. Wijffels, D. van der Veen, The role of starch as transient energy buffer in synchronized microalgal growth in *Acutodesmus obliquus*, *Algal Res.* 25 (2017) 160–167, <https://doi.org/10.1016/j.algal.2017.05.018>.
- [21] I.M. Remmers, D.E. Martens, R.H. Wijffels, P.P. Lamers, Dynamics of triacylglycerol and EPA production in *Phaeodactylum tricorutum* under nitrogen starvation at different light intensities, *PLoS One* 12 (2017) 1–13, <https://doi.org/10.1371/journal.pone.0175630>.
- [22] H.-P. Dong, E. Williams, D. Wang, Z.-X. Xie, R. Hsia, A. Jenck, R. Halden, J. Li, F. Chen, A.R. Place, Responses of *Nannochloropsis oceanica* IMET1 to long-term nitrogen starvation and recovery, *Plant Physiol.* 162 (2013) 1110–1126, <https://doi.org/10.1104/pp.113.214320>.
- [23] Y. Meng, J. Jiang, H. Wang, X. Cao, S. Xue, Q. Yang, W. Wang, The characteristics of TAG and EPA accumulation in *Nannochloropsis oceanica* IMET1 under different nitrogen supply regimes, *Bioresour. Technol.* 179 (2015) 483–489, <https://doi.org/10.1016/j.biortech.2014.12.012>.
- [24] B. Han, M. Virtanen, J. Koponen, M. Stražkraba, Effect of photoinhibition on algal photosynthesis: a dynamic model, *J. Plankton Res.* 22 (2000) 865–885.
- [25] F.C. Rubio, F.G. Camacho, J.M.F. Sevilla, Y. Chisti, E.M. Grima, A mechanistic model of photosynthesis in microalgae, *Biotechnol. Bioeng.* 81 (2003) 459–473, <https://doi.org/10.1002/bit.10492>.
- [26] A. Meneghesso, D. Simionato, C. Gerotto, N. La, G. Finazzi, T. Morosinotto, Photoacclimation of photosynthesis in the Eustigmatophycean *Nannochloropsis gaditana*, *Photosynth. Res.* 129 (2016) 291–305, <https://doi.org/10.1007/s11210-016-0297-z>.